# Threshold photoelectron spectrum of HOBr

B. Ruscic and J. Berkowitz
*Chemistry Division, Argonne National Laboratory, Argonne, Illinois 60439*

(Received 3 August 1994; accepted 23 August 1994)

The threshold photoelectron spectrum (TPES) of HOBr has been obtained in the wavelength regions corresponding to the first and second ionization bands. The adiabatic ionization potential (IP) is 10.642±0.005 eV; the O–Br stretching frequency in this $X\ ^2A''$ state is found to be 730±20 $cm^{-1}$. The adiabatic IP for the first excited state ($A\ ^2A'$) of $HOBr^+$ is 11.448±0.005 eV. The latter value confirms an earlier, tentative conclusion based on the interpretation of autoionizing structure in the photoionization mass spectrum (PIMS). There is a slight difference in the TPES and PIMS values of the first adiabatic IP, whose origin is still somewhat ambiguous. © *1994 American Institute of Physics.*

## I. INTRODUCTION

Whereas photoionization mass spectrometry (PIMS) establishes the mass of a photoion and offers a means of determining the ionization potential (IP), it is often unable to provide spectroscopic or structural information on the cation. Photoelectron spectroscopy (PES) can be interpreted to yield such information, when vibrational resolution is effected and Franck–Condon analysis can be performed. These complementary techniques are regularly employed independently for stable molecules which comprise the only, or the dominant portion of the sample. When the desired component represents a small fraction of the sample (almost invariably the case with transient species), PIMS can frequently still be effected. However, the practitioner of PES, without the benefit of mass analysis, must distinguish and identify weak photoelectron signals in the presence of strong ones. This task can be facilitated by utilizing *ab initio* calculations, and low energy windows may often exist for observing features due to low IP free radicals. In general, however, some combination of mass analysis and photoelectron spectroscopy is the key to achieving the same level of information for weakly abundant species as for more stable molecules. Ideally, this could be accomplished by coincidence spectroscopy, combining the mass and ionization energy of the desired species. In practice, this may involve very low counting times, placing a burden on the long-term stability of apparatus and sample, and the sorting out of many false coincidences. Occasionally, an intermediate solution is possible. We present one such example below.

We have recently studied[1] the PIMS of HOBr. It can be prepared in the presence of a small abundance of $Br_2$ (adiabatic IP=10.615±0.005 eV),[2] even lesser amounts of $Br_2O$ (for which we currently measured an approximate adiabatic IP of 10.18 ±0.03 eV), and a preponderance of $H_2O$ (adiabatic IP=12.615 eV).[3] From step-function structure in the PIMS of HOBr near threshold, the adiabatic IP of HOBr was deduced to be 10.638±0.003 eV (slightly larger than that of $Br_2$), and the Br–O vibrational frequency of the $X\ ^2A'$ state of $HOBr^+$ was found to be 720±30 $cm^{-1}$. In addition, the autoionization structure observed was tentatively assigned to Rydberg series with overlapping vibrational progressions converging to an IP of ~11.46 eV for the $A\ ^2A'$ excited state of $HOBr^+$, with a Br–O stretching frequency of ~670 $cm^{-1}$. Our goal was to test these deductions, using photoelectron spectroscopy together with mass analysis.

## II. EXPERIMENTAL METHOD

The basic photoionization mass spectrometric apparatus, consisting of a discharge lamp generating vacuum ultraviolet (VUV) radiation between ~600 and 2000 Å, a 3 m VUV monochromator, and a quadrupole mass spectrometer, has been described previously.[4] For the present experiment, the target chamber contained a collimated hole structure on one side (for selecting near-zero energy electrons) and a wire mesh opposite this side. The collimated hole structure is sometimes referred to as a steradiancy analyzer, and has been described previously.[5] A field of 6–8 V/cm was applied across this region, directing the near-zero energy electrons through the collimated hole structure to a channeltron multiplier. The same field accelerated the ions through the wire mesh, and into the focusing lens system, quadrupole mass filter, and onto a dynode multiplier. The near-zero energy (threshold) photoelectrons could be measured in coincidence with the mass analyzed ions, and provisions were made for detecting false coincidences, but the net coincidence counts were marginally above background.

The samples of HOBr, containing a small amount of $Br_2$ and a preponderance of $H_2O$, were prepared in a manner previously described.[1] The wavelength resolution for these experiments was 0.83 Å (full width at half-maximum).

## III. EXPERIMENTAL RESULTS

We simultaneously measure the intensity of threshold electrons, denoted $e$, the intensity of mass-analyzed $HOBr^+$ ions ($I$), and the photon intensity ($\gamma$) at each wavelength. Thus, there are several ways of displaying the data, i.e., $e/\gamma$, $I/\gamma$, and $e/I$. The data are presented in two sections, corresponding to the first and second bands of $HOBr^+$.

### A. The region between 1120 Å and threshold

Figure 1(a) is the $e/\gamma$ display in this wavelength range, while Fig. 1(b) is the simultaneously measured $I/\gamma$ spectrum. The step-function onset in the $I/\gamma$ display corresponds to some portion of the fourth peak in the $e/\gamma$ spectrum. This

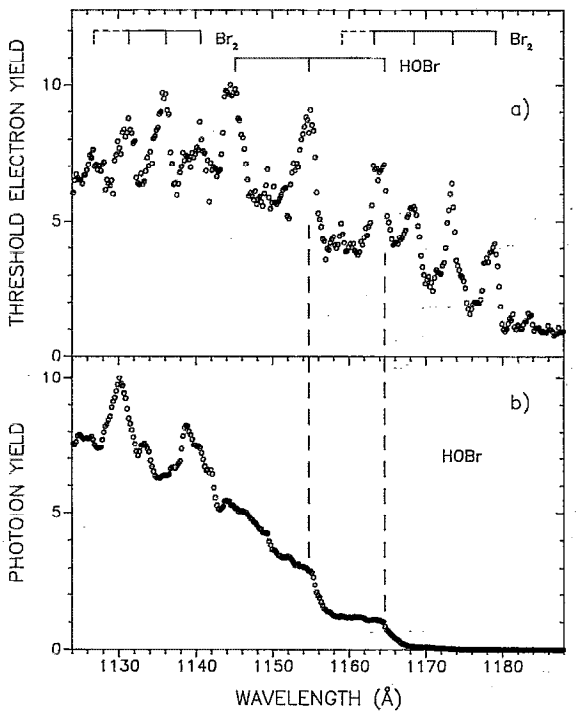


FIG. 1. (a) The threshold photoelectron spectrum ($e/\gamma$ display) of a sample containing HOBr and $Br_2$, between 1124 and 1188 Å. The sample contains a large abundance of $H_2O$, but its ionization threshold occurs at much shorter wavelength. The peaks attributable to $Br_2^+$ and $HOBr^+$ are identified in the spectrum. (b) The photoionization mass spectrum ($I/\gamma$ display) of $HOBr^+$ (HOBr) taken simultaneously with the spectrum of (a).

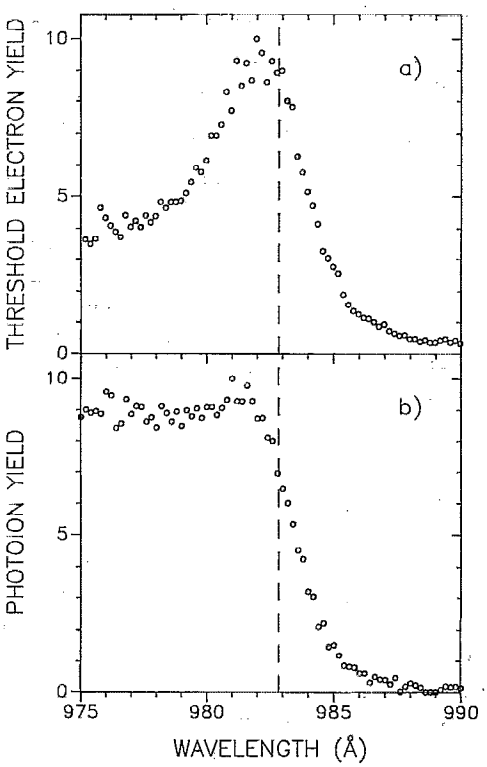


FIG. 2. (a) The threshold photoelectron spectrum of $H_2O$, obtained in the present study with the HOBr-$Br_2$-$H_2O$ sample. (b) The photoionization mass spectrum of $H_2O$ in the same wavelength range as (a). This spectrum had been obtained earlier at higher resolution (0.14 Å FWHM) (Ref. 7) but could be precisely aligned in wavelength with (a) by common calibration wavelengths. The vertical line corresponds to the currently accepted IP of $H_2O$, 12.615 eV.

fourth peak appears to manifest incipient splitting. The first three peaks, and a portion of the fourth, are vibrational components of the $X\ ^2\Pi_{3/2,g}$ state of $Br_2^+$. At the left-hand (short wavelength) side of Fig. 1(a), the vibrational components of the $^2\Pi_{1/2,g}$ state of $Br_2^+$ can be identified. Thus, fortuitously, the first band of $HOBr^+$ is straddled by the spin–orbit split components of the ground state of $Br_2^+$. We shall shortly verify these assignments, but first an aside—the interpretation of the peak shapes.

It has been demonstrated with atoms[5] that the peak shape of this threshold photoelectron spectrometer displays a sharp rise on the low energy side, whose width is governed largely by the wavelength resolution, and a tailing on the high energy side, characteristic of the collimated hole structure. With a diatomic molecule ($N_2$ was the test case), some broadening could be observed on the rapidly rising leading edge due to concomitant rotational excitations. In both monatomic and diatomic cases, it appeared as if the peak of the leading edge (not the centroid of the peak) corresponded to the spectroscopic IP. We shall interpret the $Br_2^+$ spectrum in this fashion. With triatomic molecules, particularly hydrides, one must be prepared for a more complicated peak shape. This was demonstrated by Asbrink and Rabalais[6] in a high resolution study of the first peak in the photoelectron spectrum of $H_2O$. Here, the rotational (0,0,0–0,0,0) transition was shown to correspond to a peak appearing at lower energy than the centroid of the rovibrational band. An idealized step-function photoion spectrum ($I/\gamma$ display) should be an integral of the photoelectron spectrum. Thus, if the 0,0,0–0,0,0 transition occurs at lower energy than the centroid, it should correspond to a point below the half-rise of the photoion spectrum.

Figure 2(a) is an $e/\gamma$ display of the first peak of the $H_2O^+$ spectrum, obtained in the present work. Figure 2(b) is an $I/\gamma$ spectrum of $H_2O^+$, obtained previously,[7] but with common wavelength calibrations to the present work. The point corresponding to the 0,0,0–0,0,0 transition for $H_2O^+$ at 12.615 eV≡982.8 Å is seen to be essentially the peak of the leading edge in the threshold photoelectron spectrum (TPES) [Fig. 2(a)] but on the *high energy* side of the half-rise in the $I/\gamma$ spectrum [Fig. 2(b)], rather than the expected low energy side. It is not clear why this is so, but the implication is that photoions are formed at the low energy side of threshold for which corresponding photoelectrons are not detected. Photoions deriving from high Rydberg states, which may form outside the region of electron detection, either by collisions or electric fields along the ion optical path, are likely culprits. Such photoionization, ~0.5 Å below spectroscopic threshold, has often been observed by us in $I/\gamma$ studies of both atoms and molecules

Now let us return to Fig. 1. The photoelectron peaks

TABLE I. Ionization energies (eV) of vibrational components for $Br_2 \rightarrow Br_2^+$, $X\ ^2\Pi_{g,3/2}$ and $^2\Pi_{g,1/2}$.

| $v'$ | Present value | Previous results |
|---|---|---|
| A. $Br_2 \rightarrow Br_2^+$, $X\ ^2\Pi_{g,3/2}$ | | |
| 0 | 10.516±0.005 | 10.515±0.005[a] |
| 1 | 10.566 | 10.560[b] |
| 2 | 10.611 | 10.605[b] |
| 3 | 10.659 | 10.649[b] |
| 4 | (10.697) | 10.693[b] |
| B. $Br_2 \rightarrow Br_2^+$, $^2\Pi_{g,1/2}$ | | |
| 0 | 10.870 | 10.865±0.005[a] |
| 1 | 10.913 | 10.910[b] |
| 2 | 10.959 | 10.954[b] |
| 3 | (11.003) | 10.998[b] |

[a]From Ref. 2.
[b]From $\omega_e$ and $\omega_e x_e$ values given in Ref. 8, and the adiabatic IP's given in Ref. 2.

attributed to $Br_2^+$ in Fig. 1(a) are listed in Table I, and compared with literature values.[2,8] The agreement is seen to be quite satisfactory, verifying our assignments of these peaks. The present values appear to be systematically higher than the previous literature results, by an average of 0.005 eV.

If we utilize the same method for choosing the 0,0.0–0.0,0 transition for $HOBr^+$ as was done for $H_2O^+$ and $Br_2^+$ in their threshold photoelectron spectra, i.e., selecting the point corresponding to the peak of the leading edge, we arrive at values for the vibrational components of HOBr ($^1A'$) $\rightarrow HOBr^+$ ($^2A''$) given in Table II. For the $v'=0$ component, this yields 1164.6 Å≡10.646 eV. Assuming that the combination of calibration error and point selection amounts to 0.005 eV, and that the current value may be too high, we arrive at IP (HOBr)=10.641 eV, which appears to be close to the previously deduced value based on PIMS, (1) 10.638 ±0.003 eV. However, the present TPES value [$e/\gamma$ display, Fig. 1(a)] corresponds to almost the full rise of this first step. This offset between the TPES peak and the half-rise of the PIMS step is reminiscent of our observations with $H_2O$ (see above, and Fig. 2). It implies that the higher value, obtained from the TPES peak, may be the preferred one. However, some uncertainty remains, so our choice is a mean value with a somewhat expanded error bar, i.e., 10.642±0.005 eV.

## B. The region between 1050 and 1100 Å

The data in this wavelength region are presented in three displays—$e/\gamma$, $I/\gamma$, and $e/I$— in Figs. 3(a), 3(b), and 3(c), respectively. In the $e/\gamma$ spectrum of Fig. 3(a), several peaks

TABLE II. Ionization energies (eV) of vibrational components for $HOBr \rightarrow HOBr^+$, $X\ ^2A''$ as determined from Fig. 1(a).[a]

| $v'$ | Ionization energy | Vibrational gap ($cm^{-1}$) |
|---|---|---|
| 0 | 10.646±0.005 | 734±20 |
| 1 | 10.737±0.005 | 726±20 |
| 2 | 10.827±0.005 | |

[a]The actual value of the adiabatic IP chosen in the present work is a compromise between the TPES and PIMS values, i.e., 10.642±0.005 eV.

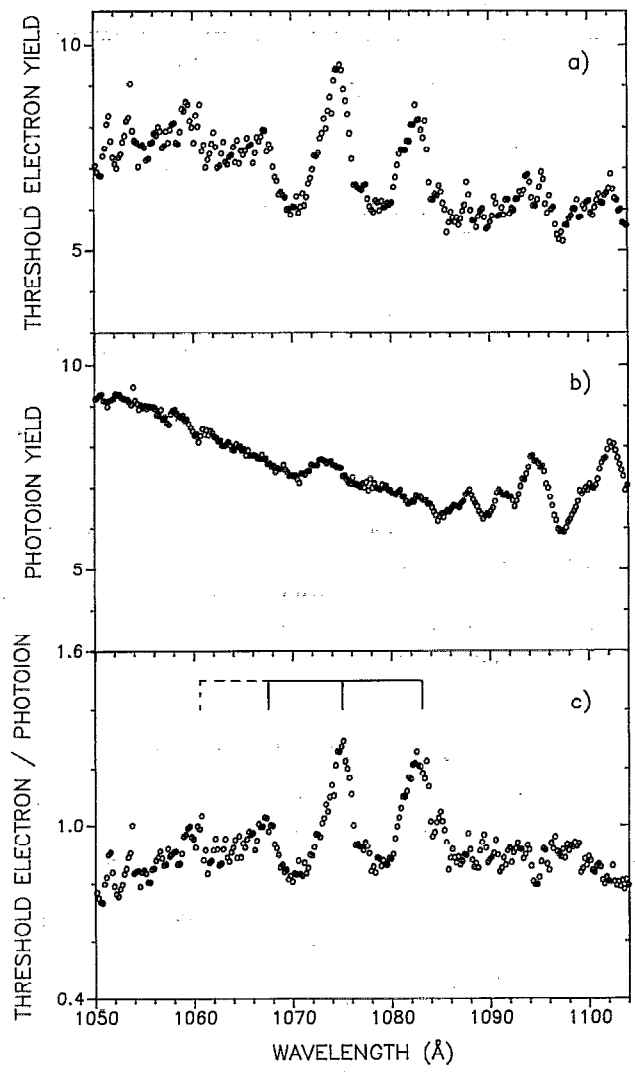


FIG. 3. (a) The TPES of the HOBr-$Br_2$ sample, between 1050 and 1104 Å. (b) The associated photoionization mass spectrum of $HOBr^+$ (HOBr). (c) The $e/I$ display of this spectrum, essentially the point-by-point division of (a) by (b). Autoionization features appearing in (a) and (b) are thereby minimized, relative to the threshold photoelectron peaks.

can be observed, with maxima at about 1060.5, 1067.5, 1075.0, 1083.0, 1094.0, 1095.3, and 1102.3 Å. The $I/\gamma$ spectrum reveals a decline between ~1050 and 1070 Å, small peaks at ~1073, 1082.5, and 1087.7 Å, and larger peaks at ~1094 and 1102 Å with high energy shoulders. Some of the autoionizing structure appearing in the $I/\gamma$ display can filter through the collimated hole structure, which does not suppress all higher energy photoelectrons.[5] A comparison of Figs. 3(a) and 3(b) shows common structure for the two bands at longest wavelength (~1094 and 1102 Å), implying that this autoionizing structure is indeed being observed in the $e/\gamma$, as well as the $I/\gamma$ spectrum. A useful tactic previously employed is to divide $e/\gamma$ by $I/\gamma$, thereby diminishing the presence of autoionization in the threshold photoelectron spectrum. In this $e/I$ display [Fig. 3(c)], the two bands at longer wavelength are largely suppressed, while the peaks at

TABLE III. Ionization energies (eV) of vibrational components for $HOBr \rightarrow HOBr^+$, $A\ ^2A'$ as determined from Fig. 3(a).

| $v'$ | Ionization energy | Vibrational gap ($cm^{-1}$) |
|---|---|---|
| 0 | 11.448±0.005 | |
| | | 687±30 |
| 1 | 11.534±0.005 | |
| | | 654±30 |
| 2 | 11.615±0.005 | |
| | | (620±40)[a] |
| 3 | (11.691±0.008)[a] | |

[a]The values in parentheses are less certain.

~1083 and 1075 Å appear prominently, and seem to be better resolved. A third peak is also more apparent at ~1067.5 Å, and possibly a fourth at ~1060.5 Å.

The prominent peaks surviving in the *e/I* display are attributed to the second ionization band, i.e., $HOBr \rightarrow HOBr^+$, $A\ ^2A'$. The energies of the vibrational components are given in Table III. The spacing of these vibrational components, reflecting the frequency and perhaps the anharmonicity of the $A'$ state, are 687±30, 654±30, and 620±40 $cm^{-1}$. Such a frequency, characteristic of an O–Br stretch, is larger than the corresponding value in neutral HOBr (620 $cm^{-1}$) but smaller than that in the ground state of the cation (730±20 $cm^{-1}$), as given in Table II.

### C. Search for higher ionization potentials

The ionization bands reported in Secs. III A and III B above can be viewed as photoemission from a $\pi_g$-like molecular halogen orbital, split into $A''$ and $A'$ components by the lower $C_s$ symmetry of HOBr. The next higher IP would presumably result from one of the deeper lying $\pi_u$-like components. Monks *et al.*[9] calculated an IP of 13.31 eV for the $B\ ^2A''$ state of $HOBr^+$. The corresponding state of $HOCl^+$ has been reported[10] to be 14.6 eV, although it was largely masked by the $H_2O^+$ photoelectron spectrum in this region. Consequently, the TPES of our sample was taken in the wavelength range <1000 Å (>12.4 eV). The only peaks appearing in this spectrum were readily attributable to $H_2O$. This is not surprising, since the photoion mass spectrum indicated that $H_2O^+$ was 3–4 orders of magnitude more intense than $HOBr^+$. Under these circumstances, even coincidence experiments performed with long counting times would be problematic.

## IV. DISCUSSION AND CONCLUSIONS

The adiabatic ionization potential of HOBr is found to be 10.642±0.005 eV by TPES, in fairly good agreement with that deduced from PIMS,[1] 10.638±0.003 eV. The latter was inferred from the half-rise of the first step in the PIMS curve. The present results imply that there may be extraneous processes involving high Rydberg states that contribute to PIMS, but not TPES. The spacing between vibrational components in the TPES of the first band implies an O–Br stretching frequency of 730±20 $cm^{-1}$ for the $X\ ^2A''$ state of $HOBr^+$, essentially confirming the value deduced form the step separations in the PIMS curve,[1] which yielded 720±30 $cm^{-1}$.

The TPES in a higher energy region, interpreted with the aid of an *e/I* display, yields an adiabatic ionization potential for the first excited state of $HOBr^+$ of 11.448±0.005 eV. In our earlier study of PIMS of HOBr, autoionizing structure was interpreted as an interleaving of one or more Rydberg series, each member of which included a vibrational progression. The limit of the Rydberg series was estimated to be ~11.46 eV, and the vibrational frequency was estimated to be ~670 $cm^{-1}$. The present results confirm the tentative conclusions deduced from the rather complex autoionizing structure.

Both the $X\ ^2A''$ and $A\ ^2A'$ states have O–Br stretching frequencies larger than in neutral HOBr. This is the behavior anticipated from emission of an electron in an antibonding, $\pi_g$-like orbital. The separation between the adiabatic IPs of the $X$ and $A$ states is found to be 0.806±0.007 eV. The *ab initio* calculations of Monks *et al.*[9] determined this energy difference to be 0.903 eV "at the cation geometry" or 0.822 eV for the neutral geometry, the latter presumably equivalent to a difference in vertical ionization potentials.

With the $X\ ^2A''$–$A\ ^2A'$ splitting in $HOBr^+$ now more firmly established, the previously performed[1] extrapolations to corresponding properties of $HOI^+$ are provided with a more secure foundation.

Conventional photoelectron spectroscopy, using either He I or some other line source and a dispersive analyzer, provides relative vibrational intensities from photoelectron peaks which are often reliable enough to use as a basis for Franck-Condon analysis. By contrast, the relative intensities of threshold photoelectron peaks are not as well defined. Hence, no attempt has been made here to deduce the geometrical structures of $HOBr^+$ in the $X$ and $A$ states.

## ACKNOWLEDGMENT

This work is supported by the U. S. Department of Energy, Basic Energy Sciences Division, under Contract No. W-31-109-ENG-38.

[1] B. Ruscic and J. Berkowitz, J. Chem Phys. (in press).
[2] H. van Lonkyuyzen and C. A. de Lange, Chem. Phys. **89**, 313 (1984).
[3] L. Karlsson, L. Mattson, R. Jadrny, R. G. Albridge, S. Pinchas, T. Bergmark, and K. Siegbahn, J. Chem. Phys. **62**, 4745 (1995).
[4] S. T. Gibson, J. P. Greene, and J. Berkowitz, J. Chem. Phys. **83**, 4319 (1985); J. Berkowitz, J. P. Greene, H. Cho, and B. Ruscic, *ibid.* **86**, 1235 (1987).
[5] R. Spohr, P. M. Guyon, W. A. Chupka, and J. Berkowitz, Rev. Sci. Instrum. **42**, 1872 (1972); see also B. Ruscic, M. Schwarz, and J. Berkowitz, J. Chem. Phys. **91**, 6772 (1989).
[6] L. Åsbrink and J. W. Rabalais, Chem. Phys. Lett. **12**, 182 (1971).
[7] J. Berkowitz, *Photoabsorption, Photoionization and Photoelectron Spectroscopy* (Academic, New York, 1979), p. 243.
[8] T. Harris, J. H. D. Eland, and R. P. Tuckett, J. Mol. Spectrosc. **98**, 269 (1983).
[9] P. S. Monks, L. J. Stief, M. Krauss, S. C. Kuo, and R. B. Klemm, J. Chem. Phys. **100**, 1902 (1994).
[10] D. Colbourne, D. C. Frost, C. A. McDowell, and N. P. C. Westwood, J. Chem. Phys. **68**, 3574 (1978).